Lithos 244 (2016) 30–42

Contents lists available at ScienceDirect

Lithos

journal homepage: www.elsevier.com/locate/lithos

Petrogenesis and geochemistry of the Late Carboniferous rear-arc (or back-arc) pillow basaltic lava in the Bogda Mountains, Chinese North Tianshan

Wei Xie *, Zhen-Yu Luo, Yi-Gang Xu, Yi-Bing Chen, Lu-Bing Hong, Liang Ma, Qiang Ma

State Key Laboratory of Isotope Geochemistry, Guangzhou Institute of Geochemistry, Chinese Academy of Sciences, Guangzhou 510640, PR China

ARTICLE INFO

Article history:
Received 8 July 2015
Accepted 14 November 2015
Available online 7 December 2015

Keywords:
Pillow basalt
Late Carboniferous
Chinese North Tianshan
Rear-arc

ABSTRACT

The tectonic nature of the Chinese Tianshan Orogen during the Late Paleozoic has been long disputed. With aims of providing constraints on this issue, an integrated study of geochronology and geochemistry has been carried out on the Late Carboniferous pillow basaltic lava of the Qijiagou Group from the Bogda Mountains, Chinese North Tianshan. Zircon SHRIMP U–Pb dating of a dacite ignimbrite, which is in conformable contact with the pillow lava, suggests that they were erupted at ~311 Ma. The pillow cores and rims show different petrological and geochemical characteristics, suggesting post-magmatic seafloor hydrothermal alteration. Nevertheless, both pillow cores and rims have the MORB-like Sr–Nd–Hf isotopes and arc-like trace element compositions. Clinopyroxene and plagioclase from the pillow lavas are compositionally different from those of the mafic rocks related to the Tarim mantle plume. These observations, together with the tholeiitic index (THI > 1) and the Fe/Mn ratios (53–57) of them, indicate that the Bogda pillow lavas may have been generated from a dry and depleted mantle source metasomatized by sediment-derived melts. Compared with basalts of the Izu–Bonin arc-back-arc system, the Bogda Late Carboniferous basaltic lavas show great resemblance to the Izu–Bonin rear-arc basalt (including the arc-like back-arc basalt) in terms of major and trace element and mineral compositions. It suggests that these basalts were likely formed in a rear-arc or back-arc environment.

1. Introduction

As the backbone of the Central Asian Orogenic Belt (CAOB), the Chinese Tianshan records abundant and important information concerning Phanerozoic crustal growth (Sengör et al., 1993; Wilhem et al., 2012; Windley et al., 2007; Xiao et al., 2004, 2013). The Chinese Tianshan is divided into three sub-belts, namely South, Central and North Tianshan. The E–W trending Bogda–Harlik (B–H) belt, belonging exclusively to the northern part of the Chinese North Tianshan, is an important tectonic belt between the Juggar Basin to the north and the Tu–Ha Basin to the south (Fig. 1). In this region, the tectonic situation during the Carboniferous–Permian remains debated, and suggestions include that there was 1) a Devonian–Carboniferous island arc transformed to a Permian post-collisional orogenic belt (Laurent-Charvet et al., 2003; Ma et al., 1997; Shu et al., 2011; Xiao et al., 2004; Yuan et al., 2010) or 2) a Carboniferous–Permian continental rift in association with a mantle plume (Gu et al., 2000, 2001; Xia et al., 2008, 2012). Meanwhile, the final closure timing of the Paleo-Tianshan Ocean to the north is also controversial, with at least three different opinions as to timing: a) the end of early Paleozoic (He et al., 1994), b) Devonian–Early Carboniferous (Chen et al., 2011; Han et al., 2010, 2011; Xia et al., 2008, 2012) or c) Late Carboniferous–Early Permian (ca. 300 Ma; Shu et al., 2011; Xiao et al., 2004; Yuan et al., 2010).

The basaltic rocks provide a critical geological record for unraveling regional tectonic history and testing different tectonic models. Late Carboniferous–Permian volcano-sedimentary rocks are widely exposed in the Bogda Mountains, consisting of basaltic lava, ignimbrite, breccia and volcanic clastic sedimentary rocks (Fig. 1; BGMRXUAR, 1993; Gu et al., 2001; Liang et al., 2011; Zhao et al., 2014). Among these volcanic rocks, high-Al basalt and basaltic andesite (HAB) and pillow basaltic lava are very significant. The former is generally associated with arcs or mid-ocean ridges on a global scale (e.g., Crawford et al., 1987; Eason and Sinton, 2006; Grove et al., 1988; Kuno, 1960; Ozerov, 2000; Sisson and Grove, 1993) while the latter generally represents the product of submarine eruption. Xie et al. (submitted to publication) proposed that the Bogda belt was an island arc system in Late Carboniferous given the presence of HAB in this region. In this study, we present new high-precise zircon SHRIMP U–Pb age and geochemical data for the Bogda pillow basalts. We first compare the Bogda basalts with those of the Izu–Bonin arc-back-arc system. Then we combine mineral

* Corresponding author at: State Key Laboratory of Isotope Geochemistry, Guangzhou Institute of Geochemistry, Chinese Academy of Sciences, 510640, Wushan, Guangzhou, PR China. Tel.: +86 20 85292337.
E-mail address: air_weixie@gig.ac.cn (W. Xie).

http://dx.doi.org/10.1016/j.lithos.2015.11.024
0024-4937/

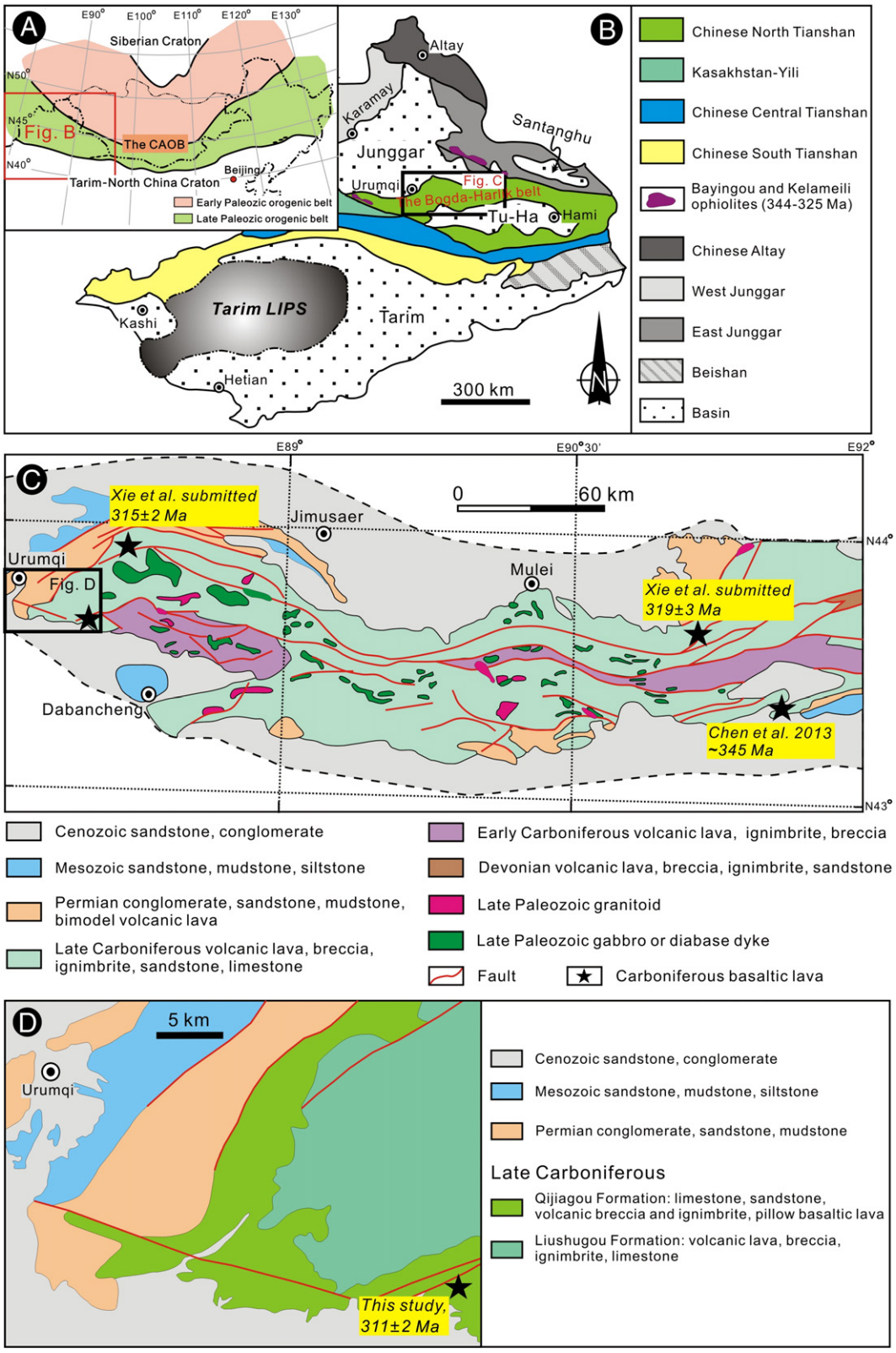

Fig. 1. A) Schematic geologic map of the Central Asian orogenic belt (CAOB); B) Simplified tectonic sketch map of most of Xinjiang province, NW China, modified after Pirajno et al. (2008), Wang et al. (2011) and Xiao et al. (2013); C) Geological map of the Bogda oregenic belt at the north margin of the Chinese North Tianshan modified after Chen et al. (2011) and Zhao et al. (2014); D) Simplified geological map around the Baiyanggou area modified after 1:200,000 Urumqi Geological Map (1965) and Shu et al. (2011).

geochemistry to constrain the petrogenesis of these rocks and their implications on the tectonic settings. Our results suggest that these Bogda Late Carboniferous basaltic lavas were likely formed in a rear-arc or back-arc environment.

2. Regional geology

The Chinese Tianshan, formed by multiple subduction–accretion and collision processes from the Neoproterozoic to the Late Paleozoic, is a

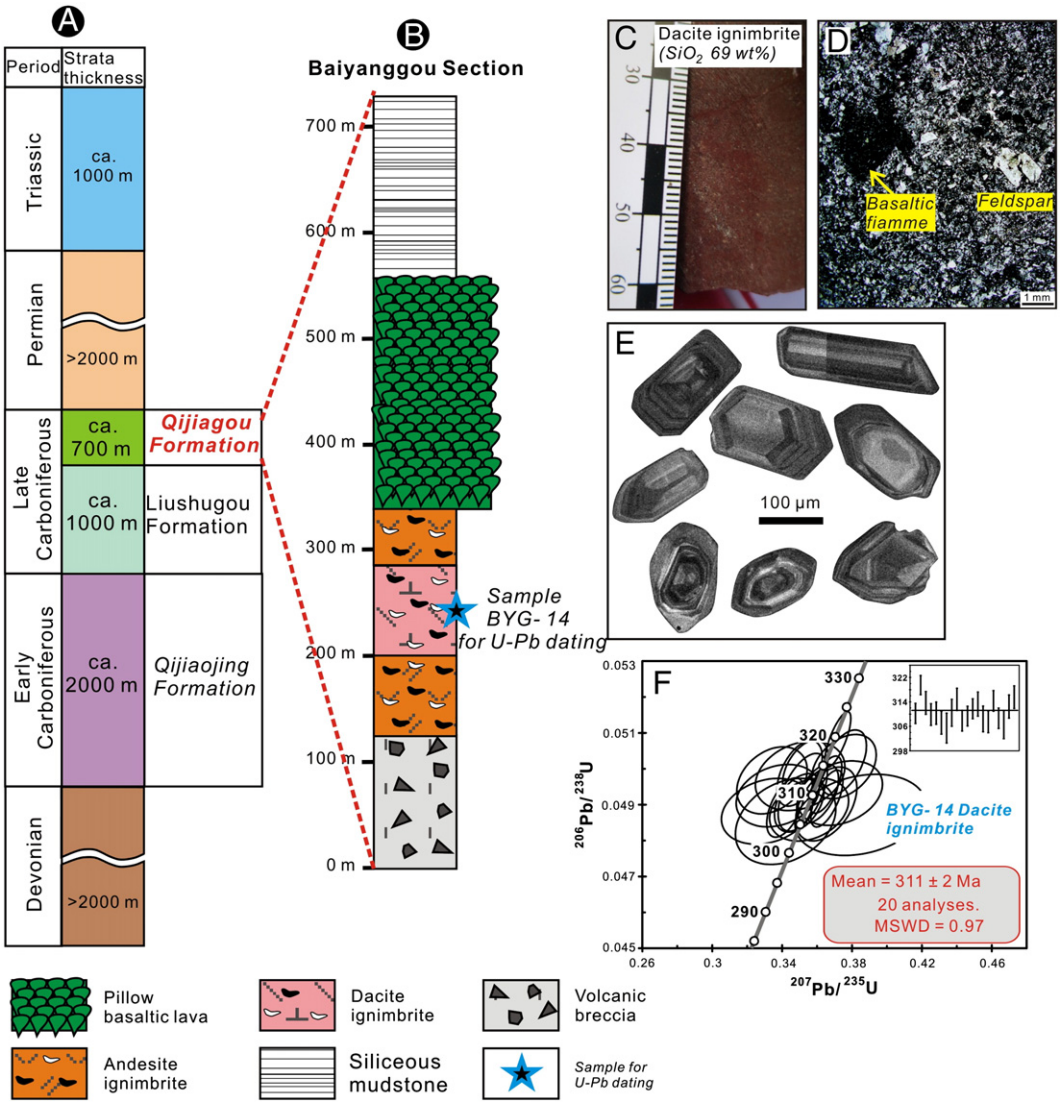

Fig. 2. (A) Simplified stratigraphic column from Devonian to Triassic for the Bogda area modified after BGMRXUAR (1993) and 1: 200,000 Urumqi Geological Map (1965). The major rock types of each period are shown in Fig. 1. (B) Baiyanggou composite detailed stratigraphy column, showing the relationship of the Bogda pillow basaltic lavas and felsic ignimbrites. The location of the Baiyanggou geological cross-section is shown in Fig. 1D. (C, D) Hand sample and Photomicrograph of the dacite ignimbrite (BYG-14) sampled for U–Pb dating; (E) CL images of representative zircons from BYG-14; (F) concordia plot of SHRIMP zircon U–Pb results for BYG-14.

complex collage of island arc assemblages, remnants of oceanic crust, continental fragments and margins (Allen et al., 1993; Sengör et al., 1993; Windley et al., 1990, 2007; Xiao et al., 2004, 2013). The Bogda–Harlik (B–H) belt that lies in the northern part of the Chinese North Tianshan contains Late Paleozoic to Quaternary sedimentary and igneous rocks. Next to the B–H belt, the Kelameili and Bayingou ophiolites crop out mainly along the Kelameili fault and the Northern Tianshan fault, respectively (Fig. 1B). The Kelameili and Bayingou ophiolites were formed during the interval 325–344 Ma (zircon U–Pb ages; Jian et al., 2005; Wang et al., 2009; Xu et al., 2006a,b). The two ophiolites are the youngest ophiolites in the Chinese Tianshan, probably representing remnants of Paleo-Tianshan Ocean (Han et al., 2010; Xiao et al., 2004, 2008). The B–H belt was considered to be a Devonian to Carboniferous island arc system, resulting from the consumption of Paleo-Tianshan Ocean (Han et al., 2010; Xiao et al., 2004, 2008; Yuan et al., 2010). In this study we focus on the Bogda belt, which is the western part of the B–H belt (Fig. 1C).

The Devonian strata in the Bogda belt are dominated by marine-terrigenous tuffaceous sandstone and volcanic rock. The Carboniferous strata are in fault contact with the Devonian rocks and are divided into three formations, namely the Lower Carboniferous Qijiaojing Formation, the Upper Carboniferous Liushugou and Qijiagou Formations (BGMRXUAR, 1993; Gu et al., 2001; Liang et al., 2011; Xia et al., 2004). The Lower and Upper Carboniferous Formations are separated by regional faults (Fig. 1C). The Lower Carboniferous Formation consists mainly of marine volcanic ignimbrite, tuffaceous sandstone, bimodal volcanic lava, while the Upper Carboniferous Formation is dominated by marine (pillow) basaltic lava and felsic ignimbrite, with minor sandstone and siltstone. The Permian strata uncomfortably overlie the Carboniferous rocks. In this region, the Permian formation is mainly composed of terrestrial conglomerate, sandstone and siliceous mudstone intercalated with bimodal volcanic lava. Jurassic clastic sediment occurs in the southeast of the study area and lies unconformably over the Permian strata (Fig. 1C; BGMRXUAR, 1993; Carroll et al., 1990).

3. Petrology of the Bogda pillow basaltic lava

At the southwest corner of the Bogda belt, one investigated stratigraphic cross-section of ~700 m thick is the Baiyanggou section (Fig. 1D). According to 1: 200,000 Urumqi Geological Map (1965), the Baiyanggou section belongs to the Upper Carboniferous Qijiagou Formation (Fig. 2). The section preserves a suite of well-exposed

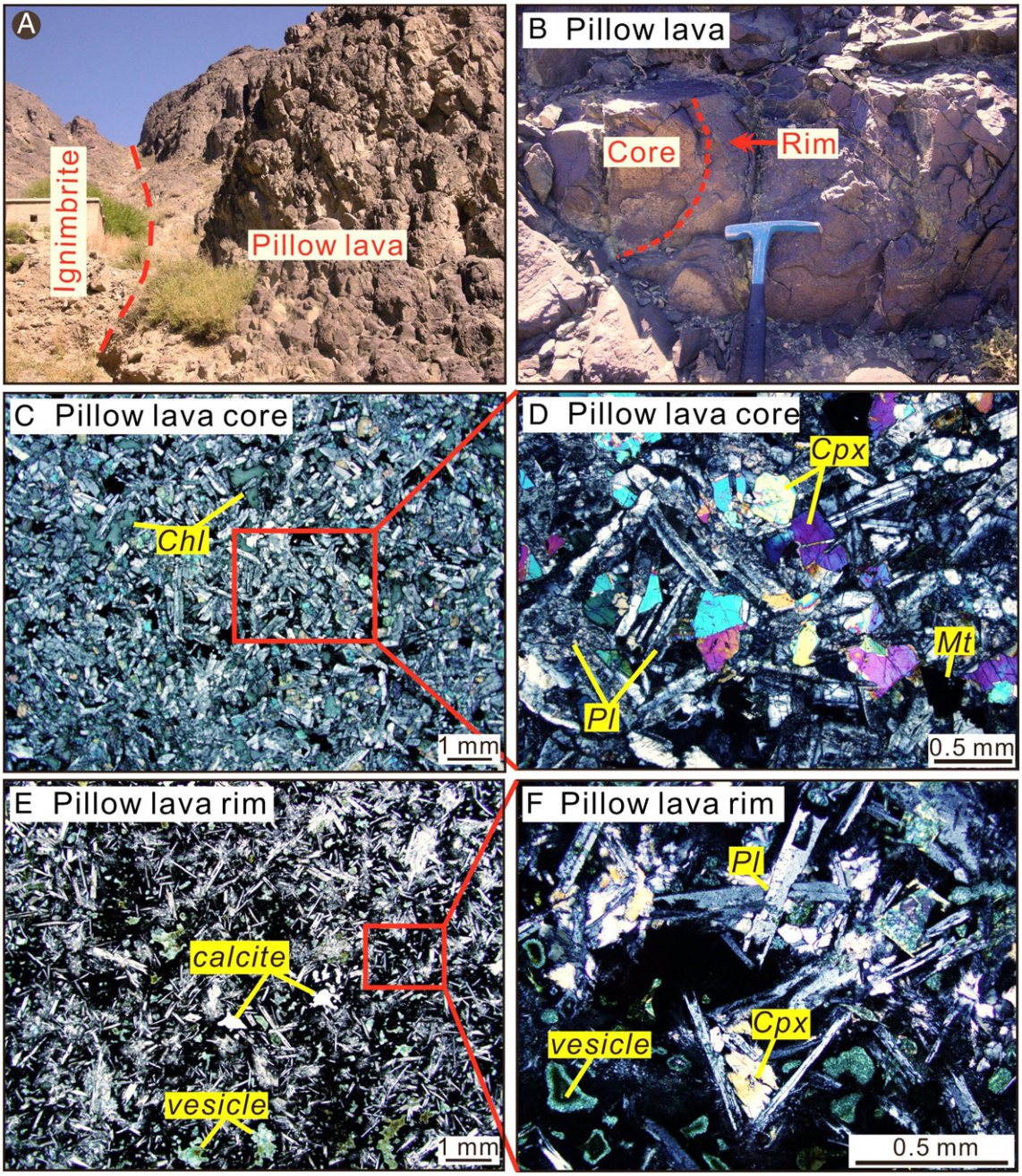

Fig. 3. (A) Field photo showing the volume and the conformable contact of the Bogda pillow basaltic lavas with the felsic ignimbrite. (B) Field photo showing the pillow core and rim. (C–F) Photomicrographs showing the pillow cores and rims. Cpx = clinopyroxene; Pl = plagioclase; Mt = magnetite; Chl = chlorite.

volcanic rocks composed of pillow basaltic lava, felsic ignimbrite and volcanic breccia. The pillow basaltic lava is ~220 m thick and overlies conformably the felsic ignimbrites (Fig. 3A). The felsic ignimbrite is about 200 m thick and is dacite and andesite in composition. They usually contain basaltic fiammes which are likely from the pillow basaltic lava (Fig. 2D). The pillows of Baiyanggou lava range from 50 to 150 cm in diameter. The boundary between the core and rim is unclear in the field but can be distinguished under microscope during systematic inspection from the core to rim. In general, the core ranges from 20 to 50 cm in radius while the concentric rim is 10–20 cm in radius (Fig. 3B).

The core and rim of the Bogda pillow lavas show different textures under microscope. The pillow core has a doleritic texture (Fig. 3C, D) and is predominantly composed of plagioclase (70–80 vol.%), clinopyroxene (10–20 vol.%) and devitrified glass matrix (<5 vol.%) with minor magnetite and sulfides. Plagioclase (0.5–1 mm) is elongated and euhedral, whereas clinopyroxene is subhedral–anhedral and filled spaces between plagioclase.

The pillow rim shows a porphyritic texture, mainly composed of microphenocrysts and dark devitrified glass matrix (Fig. 3E, F). The microphenocrysts (0.2–0.5 mm) are mainly plagioclase with minor clinopyroxene and magnetite. Generally, magnetite in pillow rim exposes more volume and smaller than the pillow core. Plagioclase shows quenched skeletal, fibrous, rosettes and swallow-tailed texture with corroded borders, whereas clinopyroxene are quenched, intergrown with closely spaced plagioclase (Fig. 3E, F). These suggest that plagioclase crystallized earlier than clinopyroxene in the Bogda pillow lavas. In addition, plagioclase and clinopyroxene in core and rim are both partially replaced by chlorite, sericite and/or epidote assemblages, but minerals in the core were suffered less intense alteration than those in the rim. Vesicle and amygdules filled with calcite and/or quartz are common in

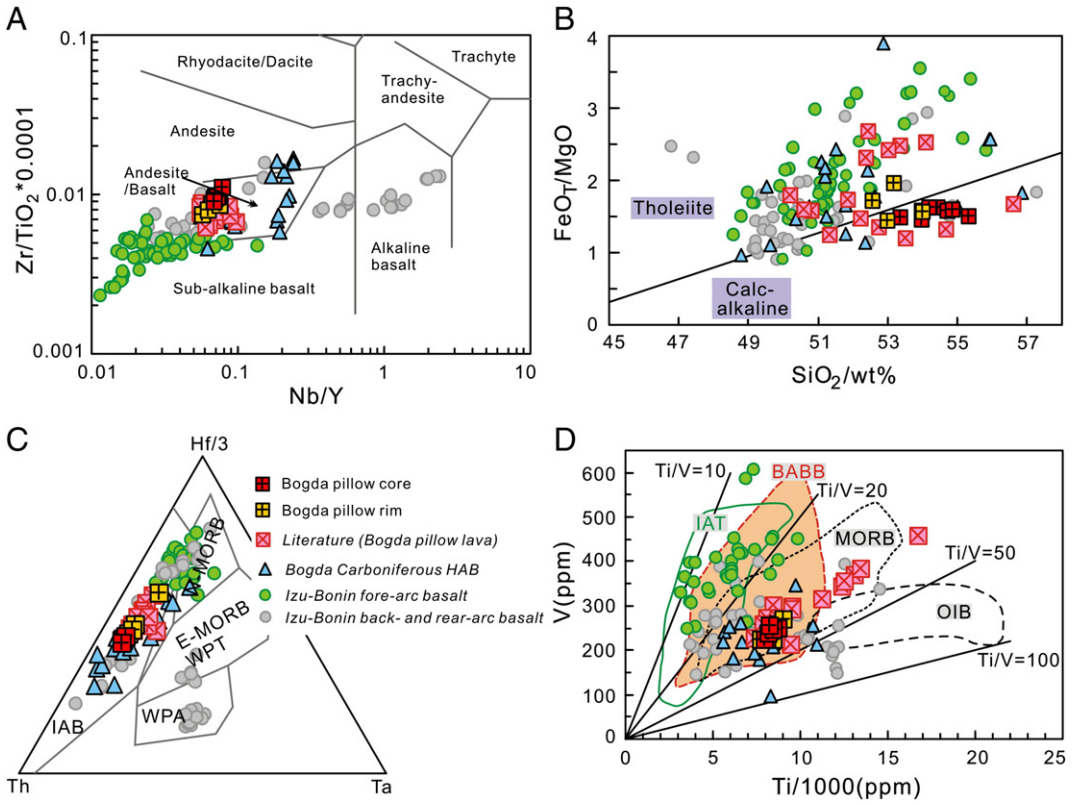

Fig. 4. Petrochemical diagrams: A) Zr/TiO_2 vs. Nb/Y (Winchester and Floyd, 1977); B) FeO_T/MgO vs. SiO_2 diagram for the sub-alkaline basaltic samples (Miyashiro, 1974); C) Th–Hf–Nb discrimination diagram (Wood, 1980); D) V versus Ti diagram (Shervais, 1982), the field of MORB, OIB, IAT (*island arc tholeiite*) and BABB (*back-arc basin basalt*) are also from Shervais (1982). Data sources: Literature data (Bogda pillow lavas) are from Xiong et al. (2010). Bogda Carboniferous HAB (*high-Al basalt and basaltic andesite*): Chen et al. (2013) and Xie et al. (submitted to publication). Izu–Bonin back- and rear-arc: Ishizuka et al. (2009). Izu–Bonin fore-arc: Reagan et al. (2010), Tamura et al. (2005), and Taylor and Nesbitt (1998).

the pillow rim and no water-rich minerals (e.g., biotite and amphibole) have been found in the Bogda pillow basaltic lavas (Fig. 3).

4. Analytical results

Analytical methods are listed in Appendix A1. Approximately 5 kg of a dacite ignimbrite (BYG-14; Fig. 2) was crushed for zircon crystal separation. Eight relatively fresh pillow core samples and four rim samples were chosen for the analysis of major and trace elements.

4.1. Zircon U–Pb age

The zircons (mostly > 100 μm) from BYG-14 exhibit mostly transparent, stubby prismatic morphologies and distinct concentric oscillatory internal structures in CL, and thus, show typical characteristics of igneous zircon. There are no inherited zircon cores (Fig. 2E). These zircons have high and scattered U and Th contents of 144–1925 ppm and 105–4070 ppm, respectively, with Th/U ratios of 0.66–2.11 (Appendix A2). Twenty analysis spots form a tight cluster on the concordia plot and yield a weighted mean $^{206}U/^{238}Pb$ age of 311 ± 2 Ma (MSWD = 0.97) (Fig. 2F). Shu et al. (2011) reported one zircon LA-ICP-MS U–Pb age of a rhyolite (297 ± 2 Ma) for a similar geological cross-section of the Bogda pillow lavas in the Baiyanggou area. Their data have relatively scattered $^{207}Pb/^{235}U$ (0.326–0.401) and show a discordant age on the concordia plot. Our new SHRIMP data with restricted $^{207}Pb/^{235}U$ (0.331–0.385) are concordant within the error range. These suggest that the Bogda pillow lavas and felsic ignimbrites from the Qijiagou Formation were mainly erupted during the Late Carboniferous (~311 Ma).

4.2. Major, trace elements and Sr, Nd, Hf, Pb isotopes

The Bogda pillow basalts have low LOI contents (1.1 to 2.6%, but 5.3% for BYG-8). In the following plots and discussion, all oxide contents of the samples have been recalculated to 100% on a volatile-free basis with all Fe as FeO (Appendix A3).

As Na_2O and K_2O might mobilize during alteration, the Zr/TiO_2 versus Nb/Y diagram (Winchester and Floyd, 1977) is utilized for rock classification. On the diagram (Fig. 4A), the Bogda pillow lavas fall in the field of sub-alkaline andesite/basalt. Th–Hf–Nb discrimination diagram further defines they are island arc basalts like the Izu–Bonin basalts (Fig. 4C). Because they straddle the line separating tholeiite and calc-alkaline affinities in Fig. 4B, we use the tholeiitic index ($THI = Fe_{4.0}/Fe_{8.0}$; Zimmer et al., 2010) to characterize the studied samples, where $Fe_{4.0}$ is the average FeO_T concentration of samples with 4 ± 1 wt.% MgO, and $Fe_{8.0}$ is the average FeO_T at 8 ± 1 wt.% MgO. According to the regression equation for MgO and FeO_T shown in Fig. 5D, the THI of the Bogda pillow lavas is 1.33, consistent with a tholeiitic affinity (THI > 1).

The Bogda pillow lavas are marked by strong enrichment in large ion lithophile elements (LILE) relative to high field-strength elements (HFSE). Furthermore, they show well-developed negative Nb–Ta and Ti anomalies and distinct positive Pb anomalies, which are similar to arc basalts worldwide and clearly distinct from ocean island basalts (OIB, Fig. 6A, B). The Bogda pillow basalts show relatively restricted ranges of total REEs (ΣREEs = 72–83) and are slightly enriched in LREEs relative to flat HREEs ($(La/Yb)_N$ = 1.6–1.9, $(Dy/Yb)_N$ = 1.1–1.2) with very slight negative Eu anomalies (δEu = 0.9–1.0).

The measured isotope ratios (Appendix A4) were corrected to 311 Ma based on Rr, Sr, Sm, Nd, Lu, Hf, U, Th and Pb contents determined by ICP–MS. The Bogda pillow lavas have low restricted

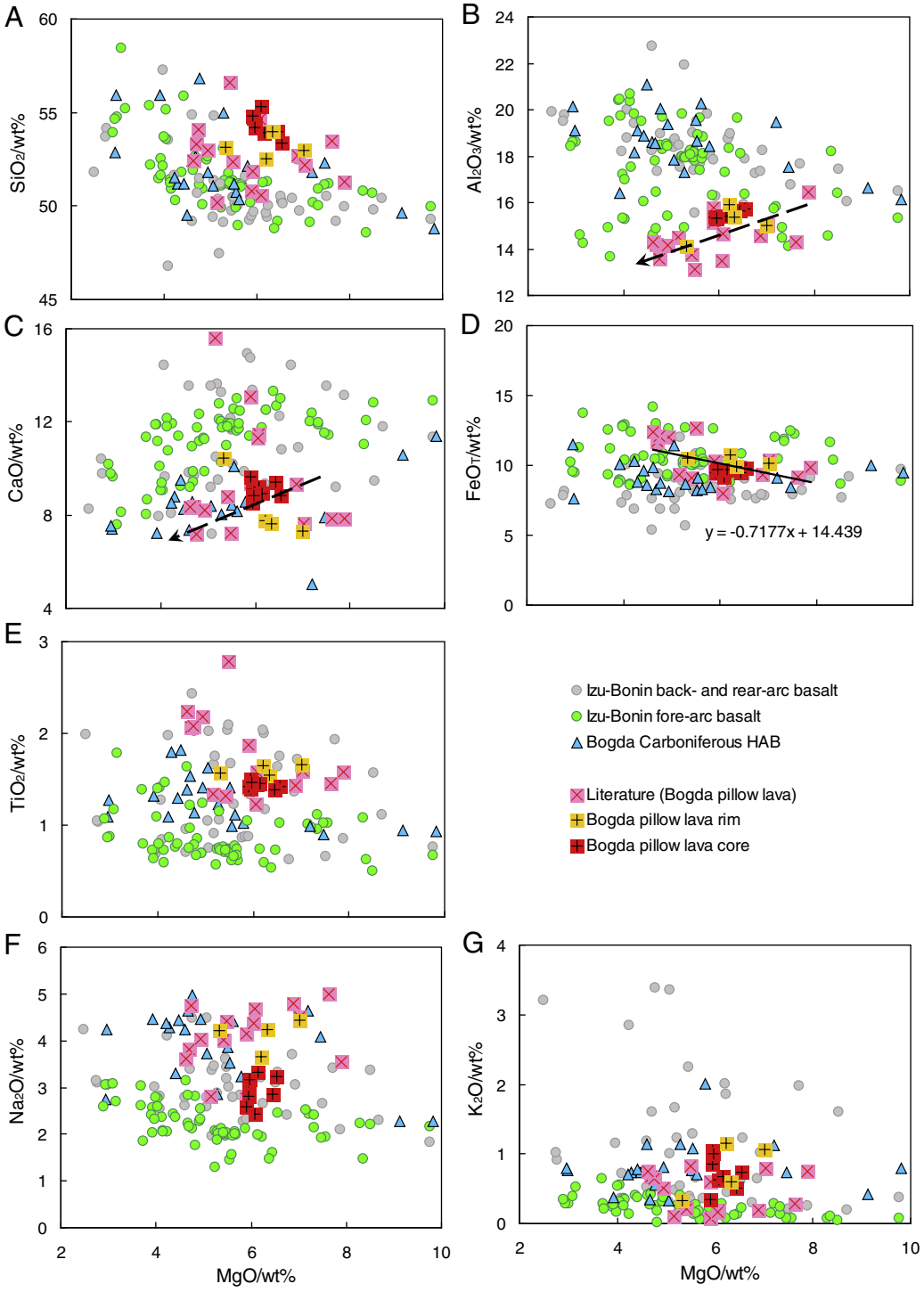

Fig. 5. Binary diagrams of oxides versus MgO. In Fig. D, the regression line ($y = -0.7177x + 14.439$) for calculating THI (tholeiitic index; Zimmer et al., 2010) is obtained after considering all of our and literature data of the Bogda pillow lavas. Data sources are the same as in Fig. 4.

initial $(^{87}Sr/^{86}Sr)_t$ ratios (0.7033 to 0.7042), quite uniform initial $(^{143}Nd/^{144}Nd)_t$ (0.512640 to 0.512718) and $(^{176}Hf/^{177}Hf)_t$ (0.282966 to 0.282982) with positive high $\varepsilon_{Nd(t)}$ (7.9 to 9.4) and $\varepsilon_{Hf(t)}$ (13.7 to 14.3). Moreover, all samples plot within the field of MORB on the $\varepsilon_{Hf(t)}$ versus $\varepsilon_{Nd(t)}$ diagram (Fig. 7B).

4.3. Mineral compositions

Major element compositions of clinopyroxene from the Bogda pillow lavas are listed in Appendix A5. All pyroxenes from the pillow core and rim are high-CaO (17–21% CaO) augite with an end-member composition of $Wo_{34-44}En_{37-50}Fs_{11-23}$ (Fig. 8A). Generally, clinopyroxenes from the Bogda pillow lavas show restricted TiO_2 (0.4–1%). Nevertheless, some spots in pillow rims have >1% TiO_2. We propose that the high TiO_2 may be due to the instrumental analyses. Because the grain size of clinopyroxene in pillow rims are too small, and they always contain a mount of smaller magnetite. Plagioclases (Pl, Appendix A6) in the Bogda pillow core are labradorite and andesine with an end-member composition of $An_{32-65}Ab_{35-66}Or_{1-2}$, whereas those in the pillow rim are albites with $An_{1-12}Ab_{83-98}Or_{0-5}$ (Fig. 8A).

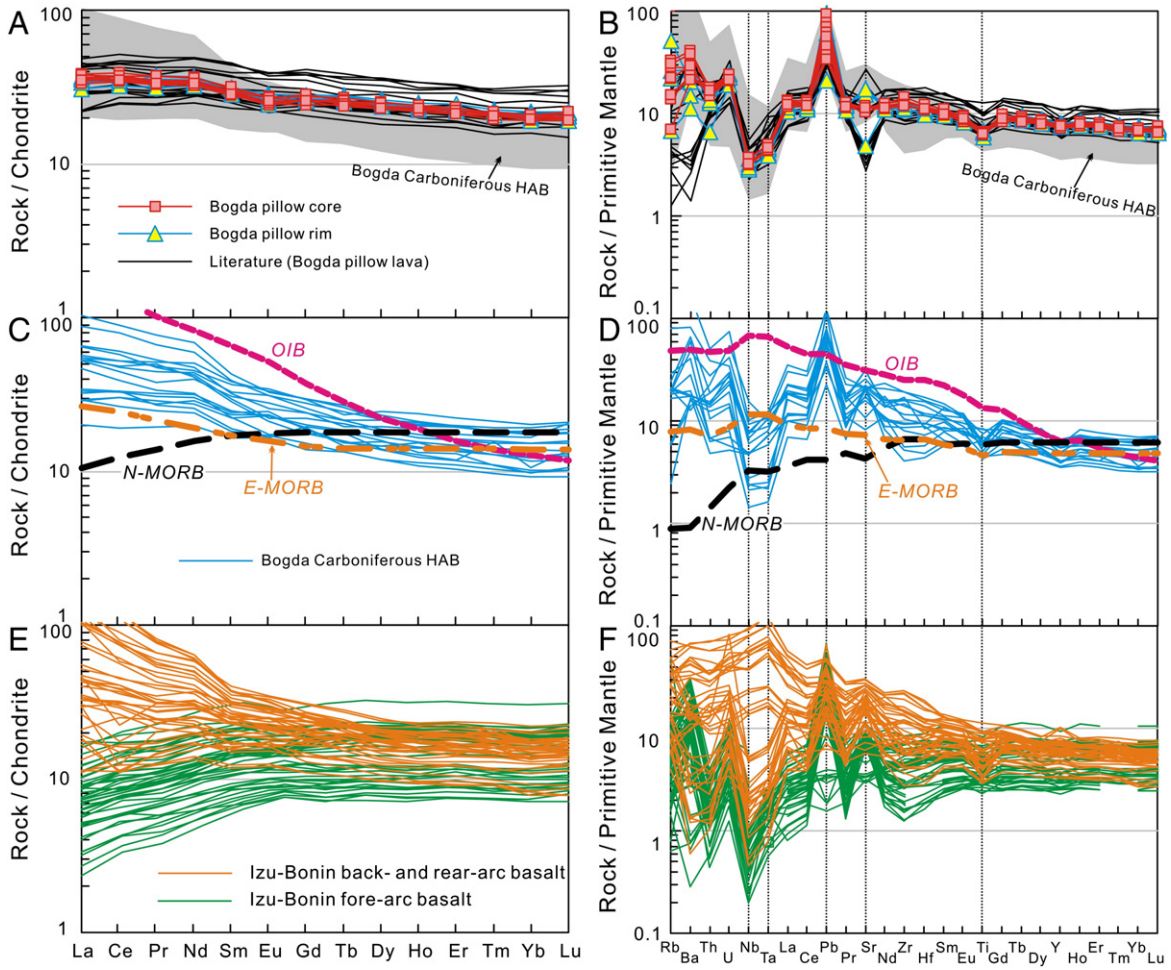

Fig. 6. Chondrite-normalized REE diagrams (A, C, E) and primitive mantle-normalized multi-element variation diagrams (B, D, F). Normalizing values, N-MORB, E-MORB and OIB are cited from Sun and McDonough (1989). Data sources are the same as in Fig. 4.

Furthermore, plagioclases from the pillow core have higher FeO (0.5–1%) than those of the pillow rim (0.1–0.4%) (except two high and scattered spots; Fig. 8C).

5. Discussion

5.1. Seafloor hydrothermal alteration

Occurrence of the pillow structure and marine Echinodermata fossil in the felsic ignimbrite (our unpublished data), indicates that the Bogda basaltic lavas were erupted in a submarine environment. Compared with the pillow core, vesicle and amygdules filled with calcite and/or quartz are common in the pillow rim (Fig. 3E, F), suggesting that the Bogda pillow lavas underwent post-magmatic seafloor hydrothermal alteration. Based on the study on the Franciscan pillow basalts in California, Swanson and Schiffman (1979) reported that pillow matrices were replaced by pumpellyite, prehnite, sphene and quartz while olivine was replaced by pumpellyite or smectite/illite, and Ca-plagioclase by albite and sericite during seafloor hydrothermal alteration. This explains the occurrence of albite in the pillow rim and labradorites and andesines in pillow core of the Bogda basalts (Fig. 8). Specifically, plagioclase and clinopyroxene in the pillow core experienced less intense alteration than those in the rim. Given the good compositional trends observed for the pillow core (Fig. 8B, C), we infer that the Bogda pillow cores underwent minor seafloor hydrothermal alteration.

Different extents of seafloor hydrothermal alteration would yield different geochemical characteristics for the rim and core of pillow basalts (Alt, 1995; Polat et al., 2003, 2012). For instance, the Bogda pillow cores show relatively restricted MgO (5.9–6.6%), Mg# (52–55), Al_2O_3 (15.4–15.8%) and Na_2O (2.4–3.3%), whereas the pillow rims have more scattered MgO (5.3–7%), Mg# (47–55), Al_2O_3 (14.1–15.9%), and especially higher Na_2O (3.7–4.4%), reflecting the effect of seafloor hydrothermal alteration (Fig. 5). The slightly higher FeO_T and TiO_2 in pillow rims may be related with more volume of magnetite in rims which might be attributed to the change of oxidation state. In terms of the trace elements, both the pillow cores and rims have restricted and similar REE, Nb, Hf, Th and even U, indicating that these elements were immobile during seafloor alteration (Figs. 6, 9). Nevertheless, the lack of correlation between the mobile elements (e.g., Rb, Ba, K, Sr, Pb) and Zr suggests that these elements were affected by seafloor alteration (Fig. 9). Hence the abundances and ratios of immobile elements are used in the following discussion. The uniform Sr–Nd–Hf isotopes indicate that these isotopes were not affected by alteration/weathering and could represent the initial values.

5.2. Rapid crystallization and crustal contamination

The gradual decrease of Al_2O_3 with decreasing MgO is consistent with fractional crystallization of plagioclase (Fig. 5B). Furthermore, the very weak negative Eu anomalies ($\delta Eu = 0.9–1.0$) do not support the accumulation or flotation of plagioclase. The low Mg# (47–55), Cr (89–139 ppm) and Ni contents (16–45 ppm) imply that the Bogda pillow lavas underwent extensive fractional crystallization of ferromagnesian minerals. Given the petrographic evidence that plagioclase

crystallized earlier than clinopyroxene in the Bogda pillow lavas, we propose that the low Mg# is attributed to extensive fractional crystallization of olivine and/or orthopyroxene. FeO_T and TiO_2 increase as MgO decreases, arguing against significant crystallization of magnetite in the Bogda pillow lavas. Like many modern pillow basalts, the Bogda pillow rim shows the black devitrified glass matrix and quenched plagioclase microphenocrysts (0.2–0.5 mm) with the skeletal, fibrous, rosettes and swallow-tailed texture (Fig. 3E, F), suggesting rapid crystallization. Although relatively intact plagioclases with the doleritic texture occur in the cores, the Bogda pillow cores have small mineral grains (<1 mm) and restricted major and trace elements, suggesting that they also likely suffered rapid crystallization.

The Bogda pillow samples have low and restricted $(^{87}Sr/^{86}Sr)_t$ ratios (0.7033–0.7042), and high $\varepsilon_{Nd(t)}$ (7.9–9.4) and $\varepsilon_{Hf(t)}$ (13.7–14.3) plotting within the field of MORB (Fig. 7). This implies that the isotope compositions of the Bogda pillow basaltic lavas were not significantly affected by crust-level processes. Thus the MORB-like Sr–Nd–Hf isotopes and arc-like trace element features of the Bogda pillow lavas are inherited their source.

5.3. Depleted mantle source modified by subduction-released fluids/melts

The Fe/Mn ratio is an important indicator of the source of basalts (e.g., Davis et al., 2013; Liu et al., 2008; Zhang et al., 2015). Four pillow rim samples have scattered Fe/Mn ratios (46–62) with variable Mg# (47–55), reflecting seafloor hydrothermal alteration. In contrast, the pillow core samples have restricted Fe/Mn ratios (53–57), which are similar to the values of MORB (55–58; Arevalo and McDonough, 2010; Liu et al., 2008; McDonough and Sun, 1995) but are lower than Hawaiian OIB (about 65–71; Humayun et al., 2004). Because olivine generally has the partition coefficient $D_{Fe/Mn} > 1$ (~1.27 in general) between mineral and liquid (e.g., Davis et al., 2013; Liu et al., 2008), crystallization of olivine could decrease the Fe/Mn ratio of residual melts. However, Sobolev et al. (2007) argued that the Fe/Mn ratio did not vary significantly with olivine fractionation (i.e., an initial Fe/Mn ratio of 63 decreases to 59 after 35% olivine crystallization from a melt derived from fertile peridotite at 4.0 GPa and 1630 °C with oxygen fugacity corresponding to QFM buffer). In contrast, because $D_{Fe/Mn}$ of clinopyroxene is <1 (~0.71 in general; Davis et al., 2013), 20% clinopyroxene crystal fractionation of MORB-like melts with initial Fe/Mn ratio of 58 and 11–15 wt.% MgO would increase the ratio to 62 (Liu et al., 2008). $D_{Fe/Mn}$ of orthopyroxene is also <1 (~0.83 in general; Davis et al., 2013) but higher than that for clinopyroxene, so the effect of orthopyroxene crystallization on the Fe/Mn ratio is minor. As Fe and Mn are incompatible in plagioclase, in theory, plagioclase crystallization has no effect on the Fe/Mn ratio. Collectively, we propose that <20% of fractional crystallization of these silicate minerals had minor influence on the Fe/Mn ratio of the pillow basalt magmas. In addition, experimental studies have shown that high Fe/Mn ratios (>60) in basaltic melts can be generated by partial melting of garnet pyroxenite or hydrous peridotite at high degrees of melting, whereas low Fe/Mn ratios (<60) most likely were inherited from dry peridotite (Liu et al., 2008; Wang et al., 2012). In this sense, the restricted Fe/Mn ratios (53–57) of the Bogda pillow core indicate a dry peridotite source.

The Sr–Nd–Hf isotopes and tholeiitic characteristics of the Bogda pillow lavas further support the model that they were generated from a MORB-like dry peridotite. However, the Bogda pillow samples are marked by strong enrichment in large ion lithophile elements (LILE) relative to high field-strength elements (HFSE) and well developed negative Nb–Ta and Ti anomalies and distinct positive Pb anomalies (Figs. 4C, 6), which are similar to arc basalts worldwide and the Bogda HAB (Xie et al., submitted to publication). These trace element characteristics are attributed to the addition of subducted inputs, such as slab-derived fluids and sediment-derived melts (e.g., Hawkesworth et al., 1997; Keppler, 1996; Pearce and Peate, 1995). Highly mobile elements (e.g., Rb, Sr, Ba, U) are concentrated into aqueous slab-derived fluids, whereas Th and LREE are partitioned into sediment-derived melts (Elliott et al., 1997; Hawkesworth et al., 1997; Miller et al., 1994; Singer et al., 2007). Except for the pillow rim sample BYG-11, the Bogda pillow lavas have the relatively restricted and high Th/Nb (0.46–0.61) and low U/Th (0.32–0.48), pointing to the effect of a sediment-derived component rather than of seafloor hydrothermal alteration (Fig. 10). The depleted, MORB-like Sr–Nd–Hf isotopes suggest sedimentary input to the mantle source is less than 1%. Although <1% sedimentary input has a minor effect on their Sr–Nd–Hf isotopes (Fig. 7), it controls the budget of the large ion lithophile elements (such as U, Th; Fig. 10). Collectively, we propose that the Bogda pillow lavas were likely generated from a dry peridotite that was metasomatized by a small volume of sediment-derived melt.

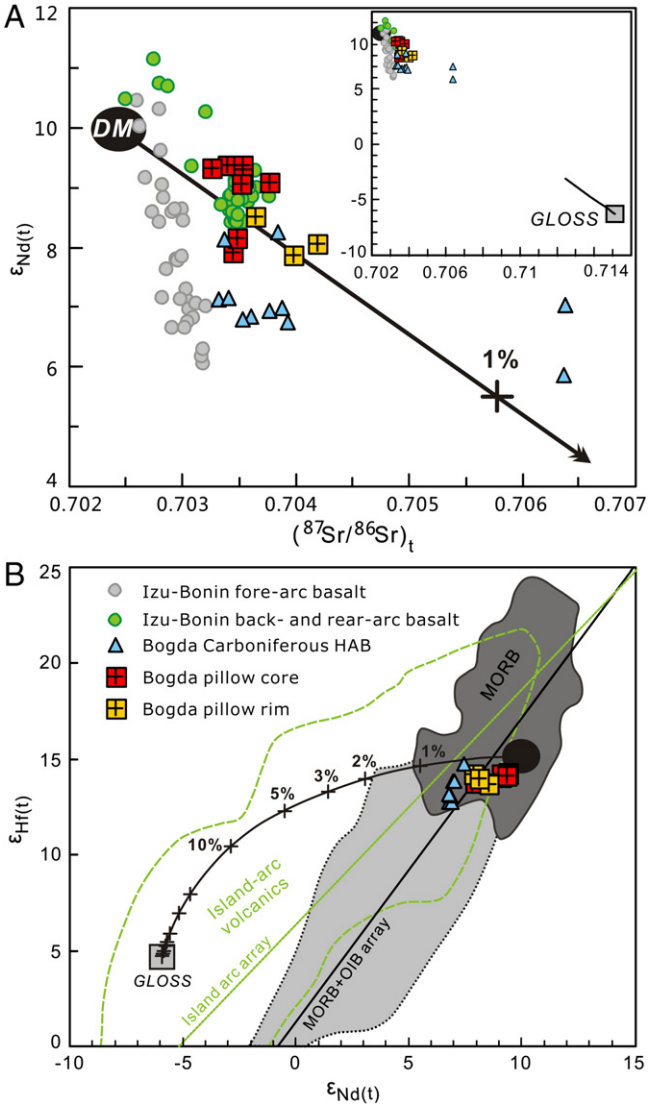

Fig. 7. Plots of initial Sr, Nd and Hf isotopic compositions. In Nd–Hf isotpe plot, the MORB + OIB and Island Arc arrays and fields for MORB, OIB, and Island arc volcanics are from Chauvel et al. (2008, 2009). The $(^{87}Sr/^{86}Sr)_t$, $\varepsilon_{Nd(t)}$ and $\varepsilon_{Hf(t)}$ values of depleted mantle (DM) are assumed as 0.7025, +10 and +15, respectively. Data sources are the same as in Fig. 4.

5.4. Magma generation and evolution

Zimmer et al. (2010) proposed to use the Tholeiitic Index (THI) to characterize magma series; magmas with THI > 1 are tholeiitic, magmas with THI < 1 are calc-alkaline. Based on the study on the Aleutian

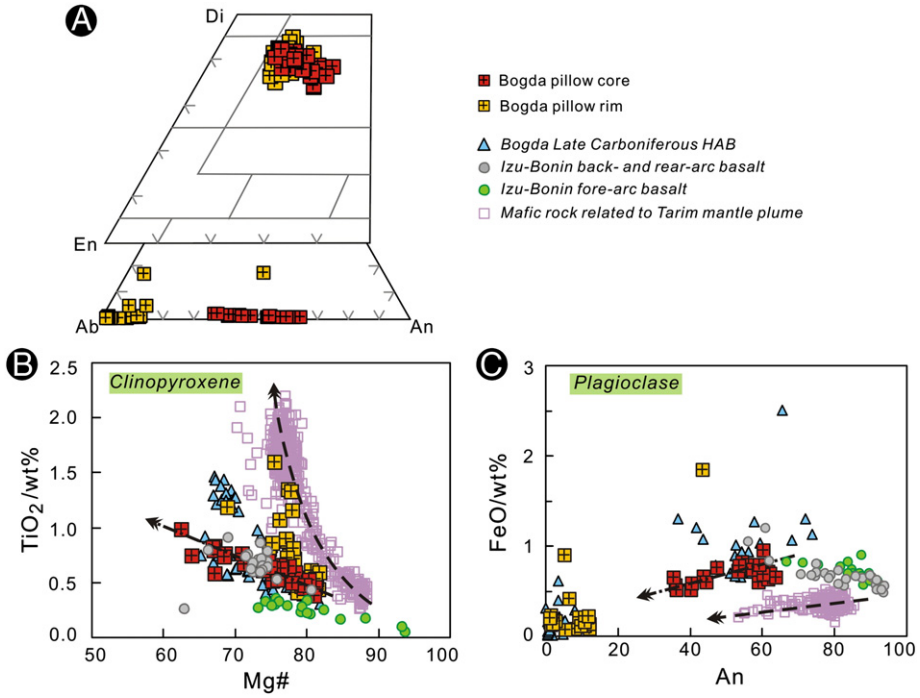

Fig. 8. (A) Diagram of normative En–Fs–Wo for clinopyroxene (Cpx) and An–Ab–Or for plagioclase (Pl). Pyroxene discrimination lines are from Poldervaart and Hess (1951). Di, diopside; En, enstatite; Ab, albite; An, anorthite. (B, C) TiO_2 vs. Mg# of clinopyroxene and FeO vs. An of plagioclase from the Bogda pillow lavas. Data sources: Bogda Late Carboniferous HAB: Xie et al. (submitted to publication). Izu–Bonin back- and rear-arc basalt: Machida and Ishii (2003). Izu–Bonin fore-arc basalt: Tamura et al. (2005). Mafic rock (wehrlite layer intrusion and basaltic dyke) related to Tarim mantle plume: Wei et al. (2014, in press).

magmas, they further provided an empirical equation for pre-eruptive magmatic water and THI:

$$X_{H2O}(\text{wt\%} \pm 1.2) = exp[(1.26 - \text{THI})/0.32]. \quad (1)$$

For the studied Bogda pillow samples, the calculated THI is 1.33 and the calculated pre-eruptive magmatic H_2O is 0.8 wt.%. Water content in arc basaltic magma can also be estimated by plagioclase–liquid hygrometer (e.g., Ushioda et al., 2014):

$$K_{D_{pl-melt}^{Ca-Na}} = 0.74X_{H2O}(\text{wt\%}) \times 100 + 0.36. \quad (2)$$

The pillow core sample BYG-4 with the highest An (64.6) plagioclase is selected to estimate the maximum water content. Although the pillow cores show a doleritic texture with ~90 vol.% plagioclase and clinopyroxene, the small mineral grains (<1 mm) and the very weak negative Eu anomalies (δEu = 0.9–1.0) do not support the accumulation or flotation of plagioclase. Thus, we assume that whole rock compositions represent liquid compositions. The estimated maximum pre-eruptive magmatic H_2O is about 0.9 wt.%. The low water content (H_2O < 1%) is in agreement with the absence of hydrous minerals (e.g., biotite and amphibole) in the Bogda pillow lavas, and further highlights their tholeiitic character.

Here, we use the clinopyroxene–liquid thermobarometers proposed by Putirka et al. (2003) to estimate the crystallization pressure, and assume that whole rock compositions represent liquid compositions. We selected the clinopyroxene with the highest MgO (16.5 wt.%) and En (46) from the magma Pulse I, as it most probably records information of the highest pressure. This clinopyroxene is assumed to be in equilibrium with the liquid as its $KD_{Fe-Mg}^{Cpx-liquid}$ falls within 0.2–0.4 (Putirka, 2008). The calculation shows that the highest crystallization pressure for the Bogda pillow lavas is 3.4 kbar, implying that the long-lived magma chamber plausibly occurred at ~11 km depth (assuming a geobarometric gradient of 3.3 km/kbar; Holdaway, 1971). A relatively deep magma chamber is also suggested for the Bogda HAB, where high pressure delayed plagioclase nucleation giving rise to the high Al content (Xie et al., submitted to publication). Together with earlier crystallization of plagioclase than clinopyroxene, the lower Al content (Al_2O_3 < 16 wt.%) of the Bogda pillow lavas suggests that they were likely generated from the shallower magma chamber compared with the Bogda HAB (Fig. 11).

5.5. Tectonic implication

The Bogda belt is an important tectonic belt separating the Juggar Basin to the north and the Turpan–Hami Basin to the south. It has been considered as 1) a Carboniferous island arc transformed to a Permian post-collisional orogenic belt (Chen et al., 2011; Ma et al., 1997; Laurent-Charvet et al., 2003; Shu et al., 2011; Xiao et al., 2004; Yuan et al., 2010), or as 2) a Carboniferous–Permian continental rift associated with a mantle plume (Gu et al., 2000, 2001; Xia et al., 2008, 2012). To further assess the nature of volcanics in the Bogda belt, Xie et al. (submitted to publication) extracted the difference between the Bogda late Carboniferous HAB and the Permian mantle plume-related basalts (e.g., the Siberia, Emeishan and Tarim traps) in detail.

The Bogda pillow basaltic lavas are also different from the mantle plume-related basalts in many aspects: 1) smaller volume (~200 m in thickness) than the mantle plume-related basalts; 2) lower TiO_2 (1.4–1.65%), FeO_T (9.5–10.7%), Nb/La (0.24–0.32) and higher $\varepsilon_{Nd(t)}$ (7.9–9.4) than the mantle plume-related basalts and mafic intrusive rocks (most TiO_2 > 1.6%; FeO_T > 10%; Nb/La > 0.5; $\varepsilon_{Nd(t)}$ < 5). In addition, most of clinopyroxenes of the Bogda pillow lavas and HAB contain lower TiO_2 than those from the Tarim large igneous province (Fig. 1B). More importantly they show distinct trends of compositional variation (Fig. 8B). As demonstrated previously, no significant crystallization of magnetite was associated with the Bogda tholeiitic pillow lavas and HAB, whereas the Tarim mafic rocks suffered the crystallization of magnetite (Wei et al., 2014, 2015). Thus, the fact of lower Ti contents in the Bogda samples than in Tarim samples cannot be related to fractionation of Ti-bearing minerals, but more likely reflects the difference of mantle

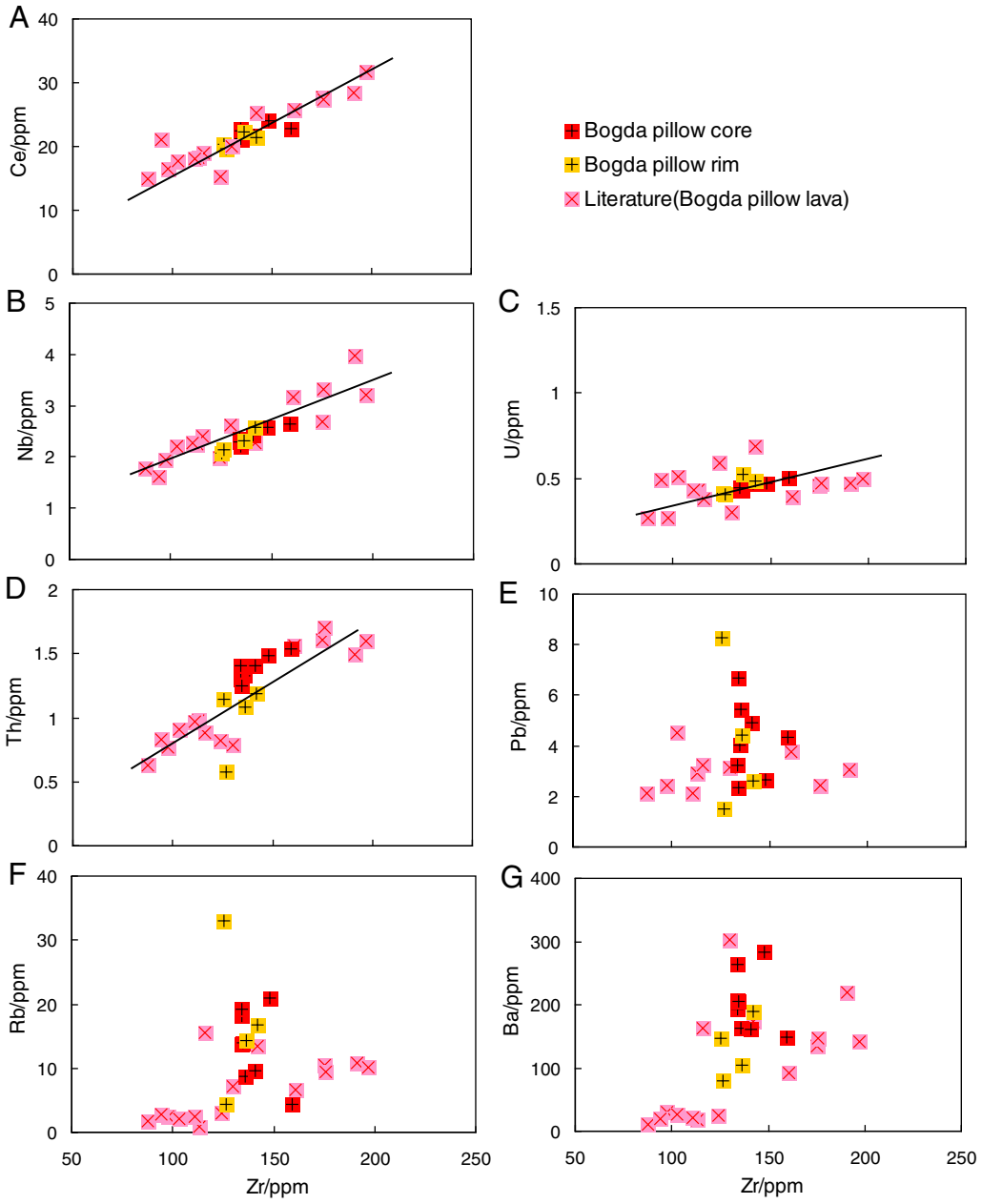

Fig. 9. Bivariate plots of trace element versus Zr to determine the extent of correlation of various immobile and mobile trace/major elements. Solid lines represent regression lines for the Bogda pillow lavas. Literature data are from Xiong et al. (2010).

source. The Bogda basalts have lower whole-rock FeO_T content than the Tarim mafic rocks but plagioclases from the former have higher FeO than the latter (Fig. 8C). Previous studies suggested that high FeO content in plagioclase might be related to high oxygen fugacity (Aigner-Torres et al., 2007; Longhi et al., 1976; Phinney, 1992; Sato, 1989). The high oxygen fugacity inferred for the Bogda basalts contrasts with the relatively low f_{O2} of the Tarim large igneous provinces (Wei et al., 2014, 2015). All these lines of evidence suggest that the "plume hypothesis" cannot adequately be applied to the Carboniferous magmatism in the Bogda belt (Xie et al., submitted to publication).

Previous studies discussed that the Bogda belt was most likely a Devonian to Carboniferous island arc system associated with south-dipping subduction of the Paleo-Tianshan Ocean (Laurent-Charvet et al., 2003; Ma et al., 1997; Xiao et al., 2004). This is further supported by occurrence of the arc-like Bogda Late Carboniferous HAB (Xie et al., submitted to publication) because arc-like HABs mostly occur in island arc settings (e.g., Crawford et al., 1987; Kuno, 1960; Ozerov, 2000; Sisson and Grove, 1993). An island arc system is generally composed of fore-arc, rear-arc and back-arc basin. Recent researches on the Izu–Bonin arc system revealed the difference between the fore-arc basalt and rear- and back-arc basalt (e.g., Ishizuka et al., 2009; Reagan et al., 2010; Tamura et al., 2005, 2007; Taylor and Nesbitt, 1998): (1) the fore-arc basalts are mostly low-K tholeiite combined with boninite and high-Mg andesite, whereas medium-K tholeiite to shoshonitic alkaline basalts are common at the rear- and back-arc system. Generally, the fore-arc tholeiitic basalts contain lower K_2O, Na_2O, Zr/Ti, Ti/V ratio than the rear- and back-arc basalts (Figs. 4, 5); (2) clinopyroxene from the fore-arc tholeiitic basalts have lower TiO_2 than those from the rear- and back-arc basalts (Fig. 8B); (3) The fore-arc basalts are strongly depleted in light rare earth elements (LREE), Nb and Th but higher U content (Fig. 10). In contrast, the rear- and back-arc basalts show LREE enrichment over HREE (Fig. 6E).

Furthermore, OIB- or E-MORB-like basalts and arc-type basalts may coexist in rear- and back-arc setting: the OIB- or E-MORB-like basalts

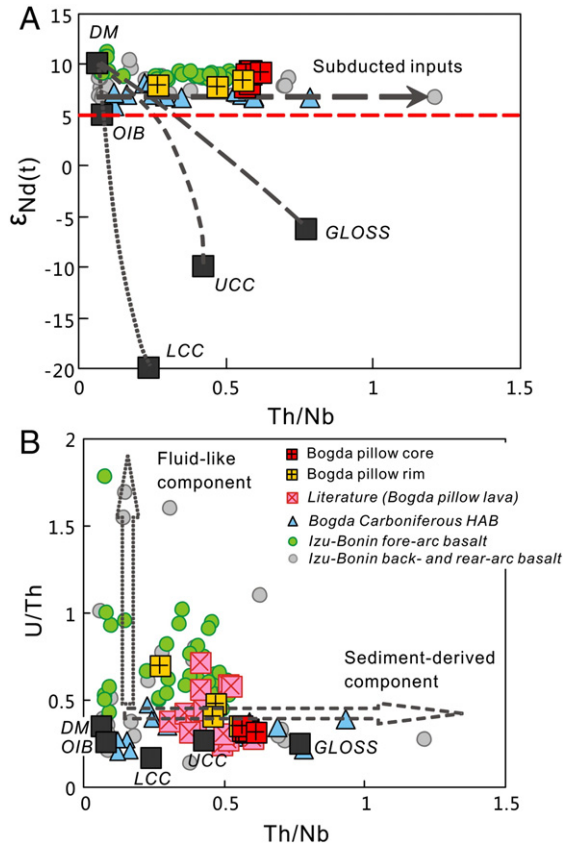

Fig. 10. (A, B) Plots of $\varepsilon_{Nd(t)}$ versus Th/Nb and Th/Nb versus U/Th. The $\varepsilon_{Nd(t)}$ values of N-MORB, OIB, UCC and LCC are assumed as +10, +5, −10 and −20, respectively. In Fig. A, the curves represent AFC (assimilation fractional crystallization) of DM with GLOSS, UCC and LCC after Xie et al. (submitted to publication). Data sources: Literature data (Bogda pillow lavas) are from Xiong et al. (2010). Bogda Carboniferous HAB (*high-Al basalt and basaltic andesite*): Chen et al. (2013) and Xie et al. (submitted to publication). Izu–Bonin back- and rear-arc: Ishizuka et al. (2009). Izu–Bonin fore-arc: Reagan et al. (2010), Tamura et al. (2005), and Taylor and Nesbitt (1998). DM (depleted mantle), OIB and GLOSS (global subducting sediment) are cited from Salters and Stracke (2004), Sun and McDonough (1989) and Plank and Langmuir (1998), respectively. UCC (upper continental crust) and LCC (lower continental crust) are from Rudnick and Gao (2005).

commonly occurs at the center of the back-arc basin and far away the rear-arc, the arc-type basalts tends to occur close to or in the rear-arc (Ishizuka et al., 2009). The difference between the fore-arc and rear-arc basalt (including the arc-like back-arc basalt) is probably due to the different subducted inputs (slab-derived fluid vs. sediment-derived melt; Ishizuka et al., 2009). In terms of major and trace element and mineral compositions, the Bogda Late Carboniferous pillow lavas and HAB show great resemblance to the Izu–Bonin rear-arc basalt (including the arc-like back-arc basalt). We therefore propose that the Bogda Late Carboniferous basaltic lavas were likely formed in a rear-arc or back-arc environment (Fig. 11).

6. Conclusions

The pillow basaltic lavas from the Upper Carboniferous Qijiagou Formation in the Bogda belt are in conformable contact with felsic ignimbrites. SHRIMP U–Pb dating on zircons of a dacite ignimbrite suggests that the Bogda pillow lavas were erupted at ~311 Ma. The pillow cores and rims show different petrographic and geochemical characteristics, reflecting post-magmatic seafloor hydrothermal alteration. However, both the cores and rims show the MORB-like Sr–Nd–Hf isotopes and arc-like trace element compositions. The THI (>1) and the Fe/Mn ratios (53–57) of the relatively fresh pillow core suggest that the Bogda lavas may have been generated from a dry and depleted mantle source metasomatized by sediment-derived melts. The Bogda Late Carboniferous pillow lavas and HAB is distinct from mantle plume-related basalts but resemble the Izu–Bonin rear-arc basalts (including the arc-like back-arc basalts). We thus propose that the Bogda Late Carboniferous basaltic lavas were likely formed in a rear-arc or back-arc environment.

Supplementary data to this article can be found online at http://dx.doi.org/10.1016/j.lithos.2015.11.024.

Acknowledgements

This study was funded by National Basic Research Program of China (2011CB808906) and GIG-CAS 135 project (Y234051001) to Yi-Gang Xu, NSFC (41503017) to Wei Xie, China Postdoctoral Science Foundation Grant (2013M542214) to Wei Xie and NSFC (41203009) to

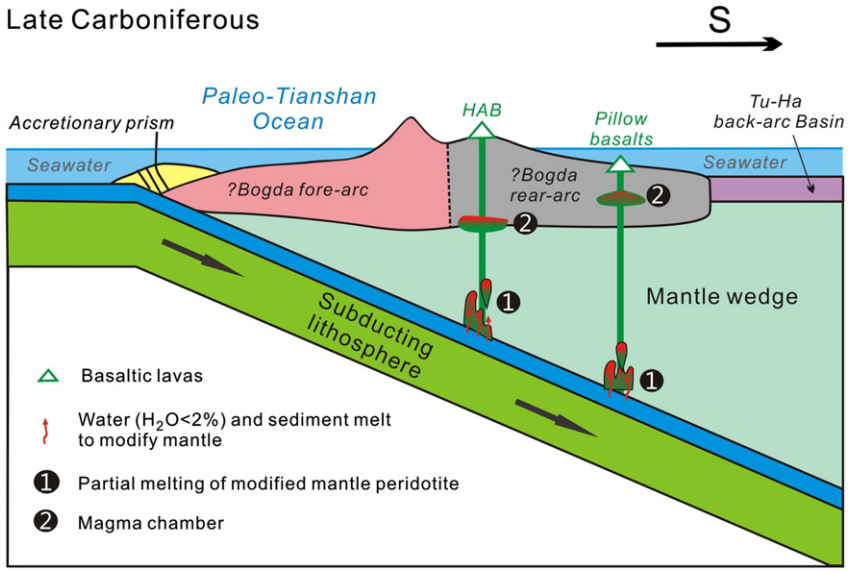

Fig. 11. Idealized schematic model for the generation of the Bogda basaltic lavas beneath the Bogda arc-back-arc system in Late Carboniferous.

Zhen-Yu Luo. We thank Hang-Qiang Xie, Yin Liu, Guang-Qian Hu, Jin-Long Ma for technical help with diverse analyses. We are grateful to the very constructive reviews of Michael Roden and an anonymous reviewer and editorial handling of Professor S-L Chung. The GIGCAS publication is No. IS-2170.

References

Aigner-Torres, M., Blundy, J., Ulmer, P., Pettke, T., 2007. Laser Ablation ICPMS study of trace element partitioning between plagioclase and basaltic melts: an experimental approach. Contributions to Mineralogy and Petrology 153, 647–667.

Allen, M.B., Windley, B.F., Zhang, C., 1993. Palaeozoic collisional tectonics and magmatism of the Chinese Tien Shan, Central Asia. Tectonophysics 220, 89–115.

Alt, J.C., 1995. Subseafloor processes in mid-ocean ridge hydrothermal systems. In: Humphris, S.E., Zierrenberg, R., Mullineaux, L., Thomson, R. (Eds.), Seafloor Hydrothermal Systems: Physical, Chemical, Biological and Geological Interactions. Geophysical Monograph 91, pp. 85–114.

Arevalo Jr., R., McDonough, W.F., 2010. Chemical variations and regional diversity observed in MORB. Chemical Geology 271, 70–85.

BGMRXUAR (Bureau of Geology and Mineral Resources of Xinjiang Uygur Autonomous Region), 1993. Regional Geology of Xinjiang Autonomous Region, Geological Memoirs, No. 32, Map Scale 1:500000. Geological Publishing House, Beijing (in Chinese).

Carroll, A.R., Liang, Y., Graham, S.A., Xiao, X., Hendrix, M.S., Chu, J., McKnigth, C.L., 1990. Junggar basin, northwestern China: trapped Late Paleozoic ocean. Tectonophysics 181, 1–14.

Chauvel, C., Lewin, E., Carpentier, M., Arndt, N.S., Marini, J.-C., 2008. Role of recycled oceanic basalt and sediment in generating the Hf–Nd mantle array. Nature Geoscience 1, 64–67.

Chauvel, C., Marini, J.-C., Plank, T., Ludden, J.N., 2009. Hf–Nd input flux in the Izu–Mariana subduction zone and recycling of subducted material in the mantle. Geochemistry, Geophysics, Geosystems 10, Q01001. http://dx.doi.org/10.1029/2008GC002101.

Chen, X., Shu, L., Santosh, M., 2011. Late Paleozoic post-collisional magmatism in the Eastern Tianshan Belt, Northwest China: new insights from geochemistry, geochronology and petrology of bimodal volcanic rocks. Lithos 127, 581–598.

Chen, X., Shu, L., Santosh, M., Zhao, X., 2013. Island arc-type bimodal magmatism in the eastern Tianshan Belt, Northwest China: geochemistry, zircon U–Pb geochronology and implications for the Paleozoic crustal evolution in Central Asia. Lithos 168–169, 48–66.

Crawford, A.J., Falloon, T.J., Eggins, S., 1987. The origin of island arc high alumina basalts. Contributions to Mineralogy and Petrology 97, 417–430.

Davis, F.A., Humayun, M., Hirschmann, M.M., Cooper, R.S., 2013. Experimentally determined mineral/melt partitioning of first-row transition elements (FRTE) during partial melting of peridotite at 3 GPa. Geochimica et Cosmochimica Acta 103, 232–260.

Eason, D., Sinton, J., 2006. Origin of high-Al N-MORB by fractional crystallization in the upper mantle beneath the Galápagos Spreading Center. Earth and Planetary Science Letters 252, 423–436.

Elliott, T., Plank, T., Zindler, A., White, W., Bourdon, B., 1997. Element transport from slab to volcanic front at the Mariana arc. Journal of Geophysical Research 102, 14991–15019.

Grove, T.L., Kinzler, R.J., Baker, M.B., Donnelly-Nolan, J.M., Lesher, C.E., 1988. Assimilation of granite by basaltic magma at Burnt Lava flow, Medicine Lake volcano, northern California: decoupling of heat and mass transfer. Contributions to Mineralogy and Petrology 99, 320–343.

Gu, L.X., Hu, S.X., Yu, C.S., Li, H.Y., Xiao, X.J., Yan, Z.F., 2000. Carboniferous volcanites in the Bogda orogenic belt of eastern Tianshan: their tectonic implications. Acta Petrologica Sinica 16, 305–316 (in Chinese with English abstract).

Gu, L.X., Hu, S.X., Yu, C.S., Zhao, M., Wu, C.Z., Li, H.Y., 2001. Intrusive activities during compression–extension tectonic conversion in the Bogda intracontinental orogen. Acta Petrologica Sinica 17, 187–198 (in Chinese with English abstract).

Han, B.-F., Guo, Z.-J., Zhang, Z.-C., Zhang, L., Chen, J.-F., Song, B., 2010. Age, geochemistry, and tectonic implications of a late Paleozoic stitching pluton in the North Tian Shan suture zone, western China. Geological Society of America Bulletin 122, 627–640.

Han, B.-F., He, G.-Q., Wang, X.-C., Guo, Z.-J., 2011. Late Carboniferous collision between the Tarim and Kazakhstan–Yili terranes in the western segment of the South Tian Shan Orogen, Central Asia, and implications for the Northern Xinjiang, western China. Earth-Science Reviews 109, 74–93.

Hawkesworth, C., Turner, S., Peate, D., McDermott, F., Calsteren, P., 1997. Elemental U and Th variations in island arc rocks: implications for U-series isotopes. Chemical Geology 139, 207–221.

He, G.Q., Li, M.S., Liu, D.Q., Tang, Y.L., Zhou, R.H., 1994. Palaeozoic Crustal Evolution and Mineralization in Xinjiang of China. Xinjiang People's Publication House, Urumqi, p. 437 (in Chinese with English abstract).

Holdaway, M.J., 1971. Stability of andalusite and the aluminum silicate phase diagram. American Journal of Science 271, 97–131.

Humayun, M., Qiu, L., Norman, M.D., 2004. Geochemical evidence for excess iron in the mantle beneath Hawaii. Science 306, 91–94.

Ishizuka, O., Yuasa, M., Taylor, R.N., Sakamoto, I., 2009. Two contrasting magmatic types coexist after the cessation of back-arc spreading. Chemical Geology 266, 274–296.

Jian, P., Liu, D.Y., Shi, Y.R., Zhang, F.Q., 2005. SHRIMP dating of SSZ ophiolites from northern Xinjiang Province, China: implications for generation of oceanic crust in the Central Asian Orogenic Belt. In: Sklyarov, E.V. (Ed.), Structural and Tectonic Correlation Across the Central Asia Orogenic Collage: North-eastern SegmentGuidebook and Abstract Volume of the Siberian Workshop IGCP-480. IEC SB RAS, Irkutsk, p. 246.

Keppler, H., 1996. Constraints from partitioning experiments on the composition of subduction-zone fluids. Nature 380, 237–240.

Kuno, H., 1960. High-alumina basalt. Journal of Petrology 1, 121–145.

Laurent-Charvet, S., Charvet, J., Monie, P., Shu, L., 2003. Late Paleozoic strike-slip shear zones in eastern central Asia (NW China): new structural and geochronological data. Tectonics 22. http://dx.doi.org/10.1029/2001TC90104.

Liang, T., Guo, X., Gao, J., Fan, T., Qin, H., Zhou, R., Hei, H., 2011. Geochemistry and structure characteristic of Carboniferous volcanic rocks in the eastern of Bogeda Mountain. Xinjiang Geology 29, 289–295 (in Chinese with English abstract).

Liu, Y., Gao, S., Kelemen, P.B., Xu, W., 2008. Recycled crust controls contrasting source compositions of Mesozoic and Cenozoic basalts in the North China Craton. Geochimica et Cosmochimica Acta 72, 2349–2376.

Longhi, J., Walker, D., Hays, J.F., 1976. Fe and Mg in plagioclase. Proceedings of Lunar Science Conference 7, 1281–1300.

Ma, R.S., Shu, L.S., Sun, J.Q., 1997. Tectonic Evolution and Metallization in the eastern Tianshan Belt, China. Geological Publish House, Beijing, p. 202 (in Chinese with English abstract).

Machida, S., Ishii, T., 2003. Backarc volcanism along the en echelon seamounts: the Enpo seamount chain in the northern Izu–Ogasawara arc. Geochemistry, Geophysics, Geosystems 4. http://dx.doi.org/10.1029/2003GC000554.

McDonough, W.F., Sun, S.S., 1995. The composition of the Earth. Chemical Geology 120, 223–253.

Miller, D.M., Goldstein, S.L., Langmuir, C.H., 1994. Cerium/lead and lead isotope ratios in arc magmas and the enrichment of lead in the continents. Nature 368, 514–520.

Miyashiro, A., 1974. Volcanic rock series in island arcs and active continental margins. American Journal of Science 274, 321–355.

Ozerov, A.Y., 2000. The evolution of high-alumina basalts of the Klyuchevskoy volcano, Kamchatka, Russia, based on microprobe analyses of mineral inclusions. Journal of Volcanology and Geothermal Research 95, 65–79.

Pearce, J.A., Peate, D.W., 1995. Tectonic implications of the composition of volcanic arc magmas. Annual Review of Earth and Planetary Sciences 23, 251–285.

Phinney, W., 1992. Partition coefficients for iron between plagioclase and basalt as a function of oxygen fugacity: implications for archean and lunar anorthosites. Geochimica et Cosmochimica Acta 56, 1885–1895.

Pirajno, F., Mao, J.W., Zhang, Z.C., Zhang, Z.H., Chai, F.M., 2008. The association of mafic–ultramafic intrusions and A-type magmatism in the Tianshan and Altay orogens, NW China: implications for geodynamic evolution and potential for the discovery of new ore deposits. Journal of Asian Earth Sciences 32, 165–183.

Plank, T., Langmuir, C.H., 1998. The chemical composition of subducting sediment and its consequences for the crust and mantle. Chemical Geology 145, 325–394.

Polat, A., Hofmann, A.W., Münker, C., Regelous, M., Appel, P.W.U., 2003. Contrasting geochemical patterns in the 3.7–3.8 Ga pillow basalt cores and rims, Isua greenstone belt, Southwest Greenland: implications for postmagmatic alteration processes. Geochimica et Cosmochimica Acta 67, 441–457.

Polat, A., Longstaffe, F., Weisener, C., Fryer, B., Frei, R., Kerrich, R., 2012. Extreme element mobility during transformation of Neoarchean (ca. 2.7 Ga) pillow basalts to a Paleoproterozoic (ca. 1.9 Ga) paleosol, Schreiber Beach, Ontario, Canada. Chemical Geology 326–327, 145–173.

Poldervaart, A., Hess, H.H., 1951. Pyroxenes in the crystallization of basaltic magma. Journal of Geology 19, 472–489.

Putirka, K.D., 2008. Thermometers and barometers for volcanic systems. Reviews in Mineralogy and Geochemistry 69, 61–120.

Putirka, K.D., Mikaelian, H., Ryerson, F., Shaw, H., 2003. New clinopyroxene–liquid thermobarometers for mafic, evolved, and volatile-bearing lava compositions, with applications to lavas from Tibet and the Snake River Plain, Idaho. American Mineralogist 88, 1542–1554.

Reagan, M.K., Ishizuka, O., Stern, R.J., Kelley, K.A., Ohara, Y., Blichert-Toft, J., Bloomer, S.H., Cash, J., Fryer, P., Hanan, B.B., Hickey-Vargas, R., Ishii, T., Kimura, J.-I., Peate, D.W., Rowe, M.C., Woods, M., 2010. Fore-arc basalts and subduction initiation in the Izu–Bonin–Mariana system. Geochemistry, Geophysics, Geosystems 11. http://dx.doi.org/10.1029/2009GC002871.

Rudnick, R.L., Gao, S., 2005. Composition of the continental crust. In: Rudnick, R.L. (Ed.), Treatise on Geochemistry. Elsevier, Amsterdam, pp. 1–64.

Salters, V.J.M., Stracke, A., 2004. Composition of the depleted mantle. Geochemistry, Geophysics, Geosystems 5. http://dx.doi.org/10.1029/2003GC000597.

Sato, H., 1989. Mg–Fe partitioning between plagioclase and liquid in basalts of hole 504B, ODP leg 111: a study of melting at 1 atm. In: Becker, K., Sakai, H., et al. (Eds.), Proceedings of the Ocean Drilling Project. scientific results 111, pp. 17–26.

Sengör, A.M.C., Natal'In, B.A., Burtman, U.S., 1993. Evolution of the Altaid tectonic collage and Palaeozoic crustal growth in Eurasia. Nature 364, 299–307.

Shervais, J.W., 1982. Ti–V plots and the petrogenesis of modern and ophiolitic lavas. Earth and Planetary Science Letters 59, 101–118.

Shu, L.S., Wang, B., Zhu, W.B., Guo, Z.J., Charvet, J., Zhang, Y., 2011. Timing of initiation of extension in the Tianshan, based on structural, geochemical and geochronological analyses of bimodal volcanism and olistostrome in the Bogda Shan (NW China). International Journal of Earth Sciences 100, 1647–1663.

Singer, B.S., Jicha, B.R., Leeman, W.P., Rogers, N.W., Thirlwall, M.F., Ryan, J., Nicolaysen, K.E., 2007. Along-strike trace element and isotopic variation in Aleutian Island Arc basalt: subduction melts sediments and dehydrates serpentine. Journal of Geophysical Research 112, B06206. http://dx.doi.org/10.1029/2006JB004897.

Sisson, T.W., Grove, T.L., 1993. Temperatures and H_2O contents of low-MgO high-alumina basalts. Contributions to Mineralogy and Petrology 113, 167–184.

Sobolev, A.V., Hofmann, A.W., Kuzmin, D.V., Yaxley, G.M., Arndt, N.T., Chung, S.L., Danyushevsky, L.V., Elliott, T., Frey, F.A., Garcia, M.O., Gurenko, A.A., Kamenetsky, V.S., Kerr, A.C., Krivolutskaya, N.A., Matvienkov, V.K., Nikogosian, I.K., Rocholl, A.,

Sigurdsson, I.A., Sushchevkaya, N.M., Teklay, M., 2007. The amount of recycled crust in sources of mantle-derived melts. Science 316, 412–417.
Sun, S.S., McDonough, W.F., 1989. Chemical and isotopic systematics of oceanic basalts: implications for mantle composition and processes. In: Saunders, A.D., Norry, M.J. (Eds.), Magmatism in the Ocean Basins. Geological Society Special Publications, pp. 313–345.
Swanson, S.E., Schiffman, P., 1979. Textural evolution and metamorphism of pillow basalts from the Franciscan Complex, Western Marin County, California. Contributions to Mineralogy and Petrology 69, 291–299.
Tamura, Y., Tani, K., Ishizuka, O., Chang, Q., Shukuno, H., Fiske, R.S., 2005. Are arc basalts dry, wet, or both? Evidence from the Sumisu caldera volcano, Izu–Bonin arc, Japan. Journal of Petrology 46, 1769–1803.
Tamura, Y., Tani, K., Chang, Q., Shukuno, H., Kawabata, H., Ishizuka, O., Fiske, R.S., 2007. Wet and dry basaltmagma evolution at Torishima Volcano, Izu–Bonin arc, Japan: the possible role of phengite in the downgoing Slab. Journal of Petrology 48, 1999–2031.
Taylor, R.N., Nesbitt, R.W., 1998. Isotopic characteristics of subduction fluids in an intraoceanic setting, Izu–Bonin Arc, Japan. Earth and Planetary Science Letters 164, 79–98.
Ushioda, M., Takahashi, E., Hamada, M., Suzuki, T., 2014. Water content in arc basaltic magma in the Northeast Japan and Izu arcs: an estimate from Ca/Na partitioning between plagioclase and melt. Earth, Planets and Space 66, 127.
Wang, B.Y., Jiang, C.Y., Li, Y.J., Wu, H.E., Xia, Z.D., Lu, R.H., 2009. Geochemistry and tectonic implications of Karamaili ophiolite in east Junggar of Xinjiang. Journal of Mineralogy and Petrology 9, 74–82 (in Chinese with English abstract).
Wang, B., Shu, L., Faure, M., Jahn, B.-m., Cluzel, D., Charvet, J., Chung, S.L., Meffre, S., 2011. Paleozoic tectonics of the southern Chinese Tianshan: insights from structural, chronological and geochemical studies of the Heiyingshan ophiolitic mélange (NW China). Tectonophysics 497, 85–104.
Wang, X.-C., Li, Z.-X., Li, X.-H., Li, J., Liu, Y., Long, W.-G., Zhou, J.-B., Wang, F., 2012. Temperature, pressure, and composition of the mantle source region of Late Cenozoic basalts in Hainan Island, SE Asia: a consequence of a young thermal mantle plume close to subduction zones? Journal of Petrology 53, 177–233.
Wei, X., Xu, Y.-G., Zhang, C.-L., Zhao, J.-X., Feng, Y.-X., 2014. Petrology and Sr–Nd isotopic disequilibrium of the Xiaohaizi intrusion, NW China: genesis of layered intrusions in the Tarim large igneous province. Journal of Petrology 55, 2567–2598.
Wei, X., Xu, Y.-G., Luo, Z.-Y., Zhao, J.-X., Feng, Y.-F., 2015. Composition of the Tarim mantle plume: constraints from clinopyroxene antecrysts in the early Permian Xiahaizi dykes, NW China. Lithos 230, 69–81.
Wilhem, C., Windley, B.F., Stampfli, G.M., 2012. The Altaids of Central Asia: a tectonic and evolutionary innovative review. Earth-Science Reviews 113, 303–341.
Winchester, J.A., Floyd, P.A., 1977. Geochemical discrimination of different magma series and their differentiation products using immobile elements. Chemical Geology 20, 325–343.
Windley, B.F., Allen, M.B., Zhang, C., Zhao, Z.Y., Wang, G.R., 1990. Paleozoic accretion and Cenozoic redeformation of the Chinese Tien Shan Range, Central Asia. Geology 18, 128–131.
Windley, B.F., Alexeiev, D., Xiao, W., Kröner, A., Badarch, G., 2007. Tectonic models for accretion of the Central Orogenic Belt. Journal of the Geological Society, London 164, 31–47.
Wood, D.A., 1980. The application of a Th–Hf–Ta diagram to problems of tectonomagmatic classification and to establishing the nature of crustal contamination of basaltic lavas of the British Tertiary volcanic province. Earth and Planetary Science Letters 50, 11–30.
Xia, L.-Q., Xia, Z.-C., Xu, X.-Y., Li, X.-M., Ma, Z.-P., Wang, L.-S., 2004. Carboniferous Tianshan igneous megaprovince and mantle plume. Geological Bulletin of China 23, 903–910 (in Chinese with English abstract).
Xia, L.-Q., Xia, Z.-C., Xu, X.-Y., Li, X.-M., Ma, Z.-P., 2008. Relative contributions of crust and mantle to the generation of the Tianshan Carboniferous rift-related basic lavas, Northwestern China. Journal of Asian Earth Sciences 31, 357–378.
Xia, L.-Q., Xu, X.-Y., Li, X.-M., Ma, Z.-P., Xia, Z.-C., 2012. Reassessment of petrogenesis of Carboniferous–Early Permian rift-related volcanic rocks in the Chinese Tianshan and its neighboring areas. Geoscience Frontiers 3, 445–471.
Xiao, W.-J., Zhang, L.-C., Qin, K.-Z., Sun, S., Li, J.-L., 2004. Paleozoic accretionary and collisional tectonics of the Eastern Tianshan (China): implications for the continental growth of Central Asia. American Journal of Science 304, 370–395.
Xiao, W., Han, C., Yuan, C., Sun, M., Lin, S., Chen, H., Li, Z., Li, J., Sun, S., 2008. Middle Cambrian to Permian subduction-related accretionary orogenesis of Northern Xinjiang, NW China: implications for the tectonic evolution of Central Asia. Journal of Asian Earth Sciences 32, 102–117.
Xiao, W., Windley, B.F., Allen, M.B., Han, C., 2013. Paleozoic multiple accretionary and collisional tectonics of the Chinese Tianshan orogenic collage. Gondwana Research 23, 1316–1341.
Xie, W., Xu, Y.-G., Chen, Y.-B., Luo Z.-Y., Hong, L.-B., High-alumina basalts from Bogda Mountains suggest an arc setting for Chinese Northern Tianshan during the Late Carboniferous, *Lithos* (submitted to publication).
Xiong, F.-H., Yang, J.-S., Yi, J., Xu, X.-Z., Chen, S.-Y., Li, T.-F., Ren, Y.-F., Zuo, G.-C., 2010. The pillow lava of Baiyanggou in Bogda, Xinjiang: geochemical and Sr–Nd–Pb isotopic characteristics. Geology in China 38, 838–853 (in Chinese with English abstract).
Xu, X., Li, X., Ma, Z., Xia, L., Xia, Z., Pen, G., 2006a. LA-ICPMS zircon U–Pb dating of gabbro from the Bayingou ophiolite in the northern Tianshan Mountains. Acta Geologica Sinica 80, 1168–1176 (in Chinese with English abstract).
Xu, X., Xia, L., Ma, Z., Wang, Y., Xia, Z., Li, X., Wang, L., 2006b. SHRIMP zircon U–Pb geochronology of the plagiogranites from Bayingou ophiolite in North Tianshan Mountains and the petrogenesis of the ophiolite. Acta Petrologica Sinica 22, 83–94 (in Chinese with English abstract).
Yuan, C., Sun, M., Wilde, S., Xiao, W.J., Xu, Y.G., Long, X.P., Zhao, G.C., 2010. Postcollisional plutons in the Balikun area, East Chinese Tianshan: evolving magmatism in response to extension and slab break-off. Lithos 119, 269–288.
Zhang, Y., Yuan, C., Sun, M., Long, X., Xia, X., Wang, X., Huang, Z., 2015. Permian doleritic dikes in the Beishan Orogenic Belt, NW China: asthenosphere–lithosphere interaction in response to slab break-off. Lithos 233, 174–192.
Zhao, T., Xu, S., Zhu, Z., Liu, X., Chen, C., 2014. Geological and geochemical features of Carboniferous volcanic rocks in Bogda–Harlik Mountains, Xinjiang and thire tectonic significance. Geological Review 60, 115–124 (in Chinese with English abstract).
Zimmer, M.M., Plank, T., Hauri, E.H., Yogodzinski, G.M., Stelling, P., Larsen, J., Singer, B., Jicha, B., Mandeville, C., Nye, C.J., 2010. The role of water in generating the calc-alkaline trend: new volatile data for Aleutian magmas and a new tholeiitic index. Journal of Petrology 51, 2411–2444.